Magnetopolaron effect on shallow donor states in GaAs

J. M. Shi, F. M. Peeters, and J. T. Devreese*
Departement Natuurkunde, Universiteit Antwerpen (UIA), Universiteitsplein 1, B-2610 Antwerpen, Belgium
(Received 11 December 1992; revised manuscript received 19 May 1993)

We report a theoretical investigation of the resonant donor magnetopolaron in GaAs. The energy levels of the ground state ($1s$-like) and eight excited states ($2s$-, $2p^{\pm}$-, $2p_z$-, $3d^{\pm 2}$-, $4f^{\pm 3}$-like) of the donor have been obtained as a function of the magnetic-field strength (B). The calculation is based on a variational approach in which we use a trial wave function with *two* variational parameters for all states but *three* for the $2s$ state. This approach gives (1) the exact energy values in the limits of $B = 0$, and (2) the energy levels that are very close to known more exact calculations at high magnetic fields. The magnetopolaron effect on these energies is studied within second-order perturbation theory. In order to explain the available experimental results it is sufficient to take into account the seven lowest donor states ($1s$, $2s$, $2p^{\pm}$, $2p_z$, $3d^{-2}$, $4f^{-3}$) and to include band nonparabolicity. Our results are in very good agreement with the available experimental data.

I. INTRODUCTION

A considerable amount of experimental and theoretical work has been carried out on GaAs. This is not only a scientifically interesting material, but also a technologically useful one.[1] A GaAs sample doped with Si is an n-type semiconductor. These Si donors are called *shallow donors* as the ionization energy of an electron bound to them ($E_b \sim 5.60$ meV) is much less than the energy gap of GaAs ($E_g = 1520$ meV). Moreover, the energy spectrum of the donor resembles closely those of a hydrogen atom.[2,3] However, a donor in GaAs has a much smaller ionization energy, and a much larger cyclotron resonance splitting than a free hydrogen atom because of the smaller effective mass of the electron and the larger relative dielectric constant of GaAs. Therefore, the shallow donor in GaAs provides a perfect laboratory for theories and experiments describing the hydrogen energy levels in intermediate and strong magnetic fields.[4] In addition to solid state systems the problem of hydrogenlike systems finds application in astrophysics and plasma physics.[5,6]

Much effort has been put into an accurate numerical calculation of the bound hydrogen states and the energy levels of the hydrogen electron in a magnetic field. The adiabatic method was the first to be employed in the high field region,[2,3,7–9] where the magnetic force on the electron is much larger than the Coulomb force, so the electron is tightly bound in the plane perpendicular to the magnetic field and comparatively weakly bound in the direction parallel to the magnetic field. The bound states are then just lying below the corresponding Landau levels of a free electron. Calculations based on this method have usually been restricted to the ground state and the first few excited states.

Perturbation theory was used by several groups who discussed the problem either in very low fields[10] or in the very high field limit,[11] and sometimes this approach was combined with the variational method.[12] With first-order and/or second-order perturbation theory using the field-free spherical hydrogenic eigenfunctions these calculations have produced accurate values for the ground state energy but less satisfactory results for the excited states.

Many authors have favored the variational method.[13–21] In the first[13] of these papers the variational trial wave functions (YKA) were relatively simple, of Gaussian shape, which gave reasonable results both for large magnetic fields and for high excited states. More recent works have used increasingly more complicated wave functions. The most comprehensive results obtained so far by the variational method were reported in Refs. 19 and 21 where a linear combination of several basis functions of identical form was used to simulate the ground state and the excited states up to the principal quantum number $n = 4$. The most accurate calculation was performed by Praddaude,[17] which can be regarded as exact[22] up to $n = 3$.

Magneto-optical studies of a variety of elemental and III-V semiconductors have revealed a multiplicity of spectral lines, which can be assigned to transitions of electrons between different states of shallow donors.[23–27] The shallow donor spectrum of n-GaAs has been studied in detail both theoretically and experimentally[28] where the measured transition energies have been explained very well with the theoretical results, but most of these experiments are done in low magnetic fields ($B < 6$ T) where the resonant electron-phonon interaction does not occur. The far-infrared studies of shallow donors in CdTe (Ref. 29) have found the polaron Zeeman effects in higher fields, which were in good agreement with a theoretical calculation.

GaAs is a polar semiconductor, so the electrostatic field of the electron will deform the crystal lattice around it. The dominant lattice modes are the longitudinal-optical (LO) phonon modes. In the center of the Brillouin zone their energy is approximately independent of the phonon wave vector. The electron with its associated

lattice deformation is called a polaron. The energy of the free polaron has been investigated extensively in the absence and in the presence of the magnetic field.[30–38] An electron bound to a donor is called a bound polaron. In Ref. 14 this polaron effect was studied for the ground state of the donor, which showed that this effect was negligible in InSb, but in Refs. 28 and 29 polaron correction to the energy levels of the shallow donor in GaAs and CdTe was shown to be important. More recently the resonant splitting of the energy levels of the donor in GaAs has been observed experimentally[39] in high magnetic fields up to $B = 23.5$ T. Resonant absorption resulting from *six* branches of the $1s \rightarrow 2p^+$ transition energies was observed. At present we are unaware of any calculation of the donor states which includes the electron-phonon interaction for states $n \geq 3$ in the resonant field region.

In this paper, we present a calculation of the transition energies $1s \rightarrow 2s$, $2p^{\pm}$, $2p_z$, $3d^{-2}$, $4f^{-3}$ for a shallow donor in GaAs in an arbitrary magnetic field. Because our ultimate aim is to compare our theoretical results with the experimental data of Refs. 28 and 39 we will follow an approach such that the effects of electron-phonon interaction and band nonparabolicity on the donor states are included as well as possible. To obtain the wave functions and energy levels of a donor electron in the absence of electron-phonon interaction, a variational form is used in which the trial wave function contains two variational parameters for all states but three for the $2s$ state. This function has an exponential form at low magnetic fields and becomes Gaussian at high magnetic fields. The effect of band nonparabolicity is included and we critically examine three different expressions of it which are present in the literature.[40–46] The polaron effect on these energy levels is calculated within second-order perturbation theory. We obtain the maximum polaron shifts to the transition energies in the nonresonant magnetic field region by formally including *all* donor states. For the polaron resonant $1s \rightarrow 2p^+$ transition we propose an approach which is able to give the correct $B \rightarrow 0$ polaron shift to the energy of the $2p^+$ state although only the following seven lowest donor states, $1s$, $2s$, $2p^{\pm}$, $2p_z$, $3d^{-2}$, and $4f^{-3}$, are taken into account. We find that the effects of polaron and band nonparabolicity have to be included in order to correctly describe the experimental transition energies.[39]

This paper is organized as follows. In Sec. II a variational calculation of the donor states is presented in the absence of electron-phonon interaction. A detailed comparison is given with previous calculations. The polaron correction to the energy levels of the donor is calculated in Sec. III. A comparison with the experimental transition energies is made in Sec. IV. Our discussions and conclusions are presented in Sec. V.

II. VARIATIONAL CALCULATION

Within the framework of an effective-mass approximation and neglecting electronic spin, a single conduction-band electron bound to a Coulombic impurity and interacting with LO phonons in a uniform magnetic field $\mathbf{B}$ is described by

$$H = H_e + H_{\mathrm{LO}} + H_I, \tag{1}$$

where H_e is the electronic part

$$H_e = \frac{1}{2m_b}\left(\mathbf{p} + \frac{e}{c}\mathbf{A}\right)^2 - \frac{e^2}{\epsilon_0 r}, \tag{2}$$

which describes a hydrogenic atom in an external magnetic field, where $\mathbf{A} = \frac{1}{2}\mathbf{B} \times \mathbf{r}$ is the vector potential of the field, c is the velocity of light in vacuum, $-e$ and m_b are the electronic charge and effective mass, and ϵ_0 is the static dielectric constant, for GaAs $m_b/m_e = 0.067$ (Ref. 47) (m_e the electronic mass in vacuum) and $\epsilon_0 = 12.75$ at liquid helium temperature.[1,39] Choosing the symmetric gauge and applying the cylindrical polar coordinate system (ρ, ϕ, z) with the magnetic field oriented along the z axis, we find

$$H_e = -\nabla^2 - \frac{2}{r} + \gamma L_z + \frac{1}{4}\gamma^2\rho^2, \tag{3}$$

where we have introduced the effective Bohr radius $a_0^* = \hbar^2\epsilon_0/m_b e^2 = 100.7$ Å as the unit of length, the effective Rydberg $R^* = e^2/2\epsilon_0 a_0^* = 5.60$ meV as the unit of energy, and $\gamma = e\hbar B/2m_b cR^* = 0.154B$ (T) as the dimensionless unit of the magnetic-field strength, $L_z = -i(\partial/\partial\phi)$ is the z component of the angular momentum operator in units of $\hbar$. The donor center is located at the origin of the coordinate system, and the position of the electron is denoted by $\mathbf{r}$. $r = (\rho^2 + z^2)^{1/2}$ is the distance between the electron and the donor center with $\rho = (x^2 + y^2)^{1/2}$ being the distance in the x-y plane.

In Eq. (1) H_{LO} is the LO phonon Hamiltonian which is given by

$$H_{\mathrm{LO}} = \sum_{\mathbf{q}} \hbar\omega_{\mathbf{q}}(a_{\mathbf{q}}^\dagger a_{\mathbf{q}} + \tfrac{1}{2}), \tag{4}$$

where $a_{\mathbf{q}}^\dagger$ ($a_{\mathbf{q}}$) is the creation (annihilation) operator of a LO phonon with wave vector $\mathbf{q}$ and frequency $\omega_{\mathbf{q}}$. For GaAs we take $\hbar\omega_{\mathbf{q}} = \hbar\omega_{\mathrm{LO}} = 36.75$ meV,[48] the value of the LO phonon energy at 4.2 K, which is the experimental region of Refs. 28 and 39.

The electron-phonon interaction in Eq. (1) is given by

$$H_I = \sum_{\mathbf{q}}(V_{\mathbf{q}} a_{\mathbf{q}} e^{i\mathbf{q}\cdot\mathbf{r}} + V_{\mathbf{q}}^* a_{\mathbf{q}}^\dagger e^{-i\mathbf{q}\cdot\mathbf{r}}), \tag{5}$$

where $V_{\mathbf{q}}$ is the Fourier coefficient of the electron-phonon interaction given by

$$|V_{\mathbf{q}}|^2 = \frac{4\pi\alpha}{\Omega}\frac{(\hbar\omega_{\mathrm{LO}})^{3/2}}{q^2}$$

with Ω the crystal volume, and

$$\alpha = \sqrt{\frac{R^*}{\hbar\omega_{\mathrm{LO}}}}\left(\frac{\epsilon_0}{\epsilon_\infty} - 1\right)$$

the standard Fröhlich coupling constant, and ϵ_∞ the high frequency dielectric constant of the material. In our calculation we take $\alpha = 0.068$ for GaAs.[47]

The Schrödinger equation with the Hamiltonian H_e cannot be solved exactly and therefore we relied on a variational approach for the donor states with trial wave functions[21]

$$|nmp\rangle = \rho^{|m|} z^p e^{im\phi} e^{-\xi\rho^2-\eta r}(1-\lambda_{2s}\sqrt{\rho^2+\sigma^2 z^2}), \quad (6)$$

which depend on the principal quantum number n, the magnetic quantum number m ($|m| < n$), and the conserved z-parity quantum number $p = 0,1$. In Eq. (6) λ_{2s} is nonzero only for the $2s$ state and is chosen such that this state is orthogonal to the ground state. The variational parameters ξ, η , and σ an additional one for the $2s$ state, are determined such that they minimize the unperturbed energy

$$E^0_{nmp} = \frac{\langle nmp|H_e|nmp\rangle}{\langle nmp|nmp\rangle}. \quad (7)$$

In the present work we included the following donor states: $1s(1,0,0)$, $2s(2,0,0)$, $2p^{\pm}(2,\pm1,0)$, $2p_z(2,0,1)$, $3d^{\pm2}(3,\pm2,0)$, and $4f^{\pm3}(4,\pm3,0)$ because they are the relevant ones for the experimental results of Refs. 28 and 39. With the above variational wave functions Eq. (6) and the Hamiltonian H_e Eq. (2) we obtained the following expressions for the diagonal matrix elements: (1) for all the states except 2s which can be reduced to a onefold numerical integral

$$\langle nmp|nmp\rangle = Q(|m|,p,0), \quad (8)$$

$$\begin{aligned}\langle nmp|H_e|nmp\rangle = {} & [\gamma m + 4\xi(|m|+1) - \eta^2]Q(|m|,p,0) + \left(\frac{\gamma^2}{4} - 4\xi^2\right)Q(|m|+1,p,0) \\ & +2pQ(|m|,p-1,0) - 4\xi\eta Q(|m|+1,p,0) - \eta Q(|m|+1,p,-3) \\ & +2[\eta(|m|+p+1)-1]Q(|m|,p,-1) - p(p+1)Q(|m|,p,-2), \end{aligned} \quad (9)$$

where we have defined the function

$$Q(i,j,k) = \frac{(-1)^i\pi(2j)!}{2^{i+2j+k}}\frac{\partial^i}{\partial\xi^i}\int_0^\infty dz\, e^{-2z(\xi z+\eta)}\frac{\partial^{2j}}{\partial(\eta+2\xi z)^{2j}}\frac{\Gamma[k+2,2z(\eta+2\xi z)]}{(\eta+2\xi z)^{k+2}}e^{2z(\eta+2\xi z)} \quad (10)$$

with $\Gamma(k,z)$ the incomplete gamma function; and (2) for the $2s$ state which involves the calculation of twofold numerical integrals

$$\langle 2s|2s\rangle = 4\pi\int_0^\infty d\rho\,\rho e^{-2\xi\rho^2}\int_0^\infty dz\, e^{-2\eta r}(1-\lambda_{2s}\sqrt{\rho^2+\sigma^2z^2})^2, \quad (11)$$

$$\begin{aligned}\langle 2s|H_e|2s\rangle \Rightarrow = {} & 4\pi\int_0^\infty d\rho\,\rho e^{-2\xi\rho^2}\int_0^\infty dz\, e^{-2\eta r}(1-\lambda_{2s}\sqrt{\rho^2+\sigma^2z^2}) \\ & \times\left\{\frac{\lambda_{2s}(\sigma^2-2\eta)}{r} + \frac{2\lambda_{2s}\rho^2(1-2\xi)}{\sqrt{\rho^2+\sigma^2z^2}}\right. \\ & \left. +(1-\lambda_{2s}\sqrt{\rho^2+\sigma^2z^2})\left[4\xi-\eta^2-\frac{2(1-\eta+2\xi\eta\rho^2)}{r}+\left(\frac{\gamma^2}{4}-4\xi^2\right)\rho^2\right]\right\}. \end{aligned} \quad (12)$$

In the present work we only need the states with $m \geq 0$ since one can easily prove the exact relation

$$E_{-|m|} = E_{|m|} - 2|m|\gamma. \quad (13)$$

In Table I we compare the results for the energies (in units of R^*) of the $1s$, $2s$, $2p_z$, $2p^+$, $3d^{+2}$, and $4f^{+3}$ states with those given by different approaches for the magnetic fields $\gamma = 0.1$, 1.0, 2.0, and 3.0. First let us compare the present results with those of YKA,[13] who used a trial wave function of the Gaussian form $\rho^{|m|}z^p\exp(im\phi - \xi\rho^2 - \eta z^2)$ to study the ground state of a hydrogenic atom. Wallis and Bowlden[49] extended this calculation to a few lowest excited states but including only one variational parameter ($\xi \equiv 1$). Here we have performed the calculation for the excited states listed in Table I with two (three for $2s$) variational parameters. It is clear that (1) our eigenvalues are generally lower except for the $2s$ and $4f^{+3}$ states in magnetic fields of $\gamma \geq 1$, and (2) the difference between these two methods decreases with increasing magnetic field and for higher excited states. The reason is that (i) the wave function should be exponential in low fields where the Coulomb potential is dominant, and Gaussian in high fields where

TABLE I. Comparison of energy spectrum (in units of R^*) of six donor states in GaAs with the results of YKA (Ref. 13), Aldrich and Greene (Ref. 19), and Praddaude (Ref. 17) for magnetic fields $\gamma = 0.1$, 1.0, 2.0, and 3.0.

γ	State	Present	YKA	Aldrich and Greene	Praddaude
	$1s$	−0.99505	−0.84443	−0.9950	−0.99505
	$2s$	−0.19609	−0.18171	−0.1960	−0.19617
0.1	$2p_z$	−0.22464	−0.20210	−0.2246	−0.22482
	$2p^+$	−0.10139	−0.07999	−0.1014	−0.10169
	$3d^{+2}$	0.22516	0.25170	0.2246	0.22433
	$4f^{+3}$	0.47735	0.47896	0.4768	
	$1s$	−0.65912	−0.52386	−0.6620	−0.66233
	$2s$	0.68900	0.68514	0.6795	0.67897
1.0	$2p_z$	0.48368	0.50807	0.4802	0.47999
	$2p^+$	2.09477	2.10809	2.0874	2.08682
	$3d^{+2}$	4.30195	4.37453	4.2945	4.29389
	$4f^{+3}$	6.40732	6.40441	6.4013	
	$1s$	−0.03525	0.09190	−0.0439	−0.04442
	$2s$	1.66738	1.65742	1.6527	1.65194
2.0	$2p_z$	1.41015	1.43955	1.4050	1.40461
	$2p^+$	4.81529	4.82510	4.8022	4.80083
	$3d^{+2}$	9.07107	9.17544	9.0586	9.05757
	$4f^{+3}$	13.20526	13.19957	13.1949	
	$1s$	0.68595	0.80911		0.67095
	$2s$	2.65321	2.64011		2.63463
3.0	$2p_z$	2.36658	2.40040		2.35996
	$2p^+$	7.61282	7.62024		7.59297
	$3d^{+2}$	13.90349	14.03309		13.88551
	$4f^{+3}$	20.05823	20.05044		

the magnetic field is dominant; (ii) the effect of the magnetic field on the higher excited states is stronger than on the lower ones so that the wave functions of these higher states change more quickly from exponential to Gaussian. A comparison with the results of Aldrich and Greene[19] leads to similar conclusions; they used a linear combination of 120 basis functions of the Gaussian form to simulate the donor states up to $n = 4$. Using an expansion of the wave function in Laguerre polynomials, Praddaude[17] obtained the highly accurate energies which are better than ours, but the errors for the binding energies of the donor states are less than 1.6% except for the $2s$ state for which it is less than 5.2% when $\gamma = 3.0$. The binding energy of the $2s$ state is given in Fig. 1 as a function of the magnetic field. We compare the present results (solid curve) with those of Makado and McGill[21] (dashed curve), Cubib, Fabri, and Fiori[16] (solid squares) and YKA (dotted curve). It is apparent that our results are very good at low magnetic fields ($\gamma < 0.4$), and become less good at high magnetic fields. It is clear from this figure that the binding energy of this state does not monotonously increase with increasing magnetic field strength. This is different from the other states whose binding energies increase with increasing field strength. The different behavior originates from the fact that the average distance between the $2s$ electron and the donor center is not a monotonously decreasing function of the magnetic field which is shown in the inset of Fig. 1.

We compare in Table II our calculated results [indicated by (a)] for the $1s \rightarrow 2p^+$ transition energy with those of YKA (b) and Praddaude (c) for the magnetic fields $\gamma = 0.1$, 1.0, 2.0, 3.0, 5.0, and 10.0. Notice that (1) the difference between the present and Praddaude's results are under 0.2% which is good enough as input for our further calculation; (2) the largest difference occurs for $\gamma \approx 1$ which is the intermediate magnetic field region where the wave function transforms from exponential to Gaussian; (3) the difference with the YKA results is larger and in low magnetic fields it is over 15%. Thus a Gaussian wave function always underestimates the transition energy. We tried to improve our theoretical results by introducing an additional variational parameter κ in Eq. (6) as Larsen did in Ref. 14 where $\exp(-\eta\sqrt{\rho^2 + z^2})$ was replaced by $\exp(-\eta\sqrt{\rho^2 + \kappa^2 z^2})$. We found that the value of the third variational parameter κ is always near 1, especially for $\gamma \rightarrow 0$ and $\gamma > 1$. Only in the intermediate magnetic field region an improvement less than 0.13% was obtained to the $1s \rightarrow 2p^+$ transition energy.

Figure 2 shows the contour maps of the electron probability density in the x-z plane for two magnetic fields: $\gamma = 0.0$ (left figures) and $\gamma = 3.0$ (right figures) for the donor states: (a) $1s$, (b) $2s$, (c) $2p^{\pm}$, (d) $2p_z$, (e) $3d^{\pm 2}$, and (f) $4f^{\pm 3}$. We notice that (1) the magnetic field compresses the wave function considerably in the x direction, that is in the x-y plane. But at the same time the wave

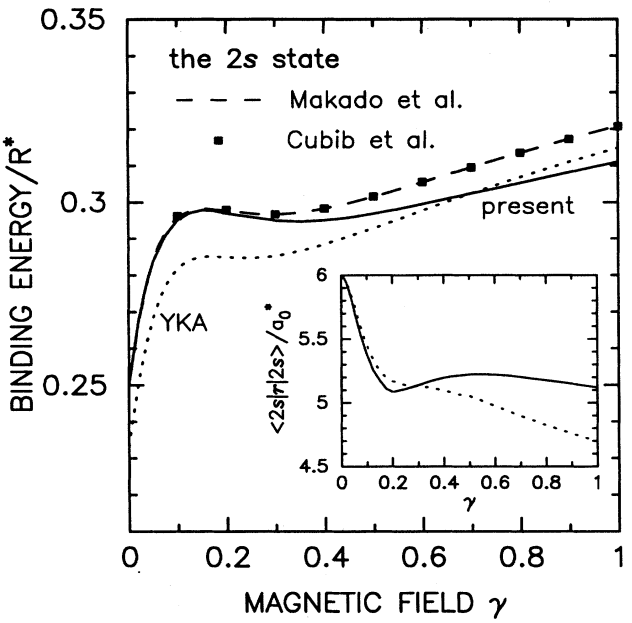

FIG. 1. The binding energy (in units of the effective Rydberg $R^* = 5.60$ meV) of the $2s$ state (solid curve) vs magnetic field $\gamma = 0.154B$ (T) compared to the corresponding result from YKA (Ref. 13) (dotted curve), Makado and McGill (Ref. 21) (dashed curve), and Cubib, Fabri, and Fiori (Ref. 16) (solid squares). The inserted figure shows the average distance (in units of the effective Bohr radius $a_0^* = 100.7$ Å) between the $2s$ electron and the donor center as a function of the magnetic field for the present and YKA's cases.

function is also compressed in the z direction. The reason is that the magnetic field confines the electron motion in the plane perpendicular to the magnetic field, thus on the average the electron is closer to the donor center and consequently the Coulomb binding energy increases, which in turn leads to a reduction of the extent of the wave function in the direction of the magnetic field; (2) the states with nonzero magnetic quantum number are more sensitive to an increase of the magnetic field than the others, and the state with odd z parity ($2p_z$) is the least sensitive; and (3) the dotted curves in (b) for the $2s$ state indicate the zero value of the wave function.

The numerical results for the widths (in units of a_0^*) of the different wave functions are given in Fig. 3 in the z direction [$\langle z^2\rangle^{1/2}$, Fig. 3(a)] and in the x-y plane [$\langle x^2+y^2\rangle^{1/2}/\sqrt{2}$, Fig. 3(b)] as a function of the magnetic field for the donor states: $1s$ (solid curves), $2s$ (thin-dashed curves), $2p^{\pm}$ (dashed curves), $2p_z$ (dash-dotted curves), $3d^{\pm 2}$ (dotted curves) and $4f^{\pm 3}$ (— · · · — curves). Notice the following: (1) the results for the states with the quantum numbers $(n,+m,p)$ and $(n,-m,p)$ share one curve, because the wave functions for both states are the same up to a phase factor; (2) all the different states become more localized with increasing magnetic field except for the $2s$ state in the z direction at low magnetic fields; (3) the states which are spread out more at $\gamma = 0$ are more sensitive to the magnetic field; (4) the $1s$ state is the most localized in all directions, and the $2s$ state is the most spread out in the z direction when $\gamma > 0.2$; and (5) the rapid increase of the width of the $2s$ state in the z direction is a consequence of the fact that the limiting shape of the nodal surface of this state for $B \to \infty$ is a pair of planes orthogonal to the z axis,[16,50] rather than a cylinder as assumed in Ref. 7, which is also apparent from Fig. 2(b).

In Figs. 4(a) and 4(b) we present the donor energy levels of the $1s$, $2s$, $2p^{\pm}$, $2p_z$, $3d^{-2}$, and $4f^{-3}$ states as a function of the magnetic field. As a reference we have also plotted the lowest two Landau levels for free electrons, i.e., $\frac{1}{2}\hbar\omega_c$ and $\frac{3}{2}\hbar\omega_c$, which are indicated by the dotted lines in Fig. 4(b). The binding energy of the donor state is given by $E_i^b = (N+\frac{1}{2})\hbar\omega_c - E_i^0$ (N is the Landau-level quantum number) with $N = 1$ for $i = 2p^+$ and $N = 0$ for the others, where $\omega_c = eB/m_bc$ is the cyclotron resonance frequency for a noninteracting electron. Notice that in the region ($\gamma < 0.6$) there are several energy-level crossings, which are given in more detail in Fig. 4(a); for example, the crossing of the $2p_z$ and $3d^{-2}$ energy levels is a consequence of the fact that the large magnetic moment of the $3d^{-2}$ state gives a large negative contribution to the energy which is absent in the $2p_z$ state.

III. ELECTRON-PHONON INTERACTION

Because GaAs is a weak polar material, we can use second-order perturbation theory to calculate the polaron correction to the energy of the ith state

TABLE II. Comparison of the $1s \to 2p^+$ transition energy (in units of R^*) for different magnetic fields. We compare the present results with those of YKA (Ref. 13) and the very accurate results of Praddaude (Ref. 17). The last two columns give the percentage difference with the present results.

	Present	YKA	Praddaude		
γ	(a)	(b)	(c)	$\frac{2(a-b)}{a+b}\%$	$\frac{2(a-c)}{a+c}\%$
0.1	0.89366	0.76444	0.89336	15.58651	0.03358
1.0	2.75389	2.63195	2.74915	4.52817	0.17227
2.0	4.85054	4.73320	4.84525	2.44873	0.10912
3.0	6.92687	6.81113	6.92202	1.68496	0.07004
5.0	11.04443	10.92910		1.04972	
10.0	21.24375	21.12543		0.55852	

$$\Delta E_i = -\sum_j \sum_{\mathbf{q}} \frac{|\langle j;\mathbf{q}|H_I|i;\mathbf{0}\rangle|^2}{\hbar\omega_{\mathbf{q}} + E_j^0 - E_i^0 - \Delta_i}, \tag{14}$$

where $\Delta_i = 0$ for all states in the polaron nonresonant region which corresponds to Rayleigh-Schrödinger perturbation theory (RSPT), and $\Delta_{2p^+} = \Delta E_{2p^+} - \Delta E_{1s}$ for the $2p^+$ state which corresponds to the improved Wigner-Brillouin-perturbation theory (IWBPT).[32,43,51] $|j;\mathbf{q}\rangle$ describes a state composed of a donor electron with unperturbed energy E_j^0 and a LO phonon with momentum $\hbar\mathbf{q} = \hbar(\mathbf{q}_\parallel, q_z)$ and energy $\hbar\omega_{\mathbf{q}}$. In our calculation we have assumed that the energy of the LO phonon $\hbar\omega_{\mathbf{q}} = \hbar\omega_{\mathrm{LO}}$ is independent of its wave vector, and consequently the matrix elements of the electron-phonon interaction, $H_I^{i,j} = \sum_{\mathbf{q}} |\langle j;\mathbf{q}|H_I|i;\mathbf{0}\rangle|^2$, are given by

$$\begin{aligned} H_I^{i,j} = & \frac{32\pi\alpha(\hbar\omega_{LO})^{3/2}}{\langle n_i m_i p_i|n_i m_i p_i\rangle\langle n_j m_j p_j|n_j m_j p_j\rangle} \int_0^\infty dq_\parallel q_\parallel \int_0^\infty dq_z \frac{1}{q_\parallel^2 + q_z^2} \\ & \times |G(2+|m_i|+|m_j|, |m_i - m_j|, p_i + p_j, \xi_i + \xi_j, \eta_i + \eta_j; q_\parallel, q_z) \\ & + \lambda_{2s}^2 [G(4,0,0,2\xi_{2s}, 2\eta_{2s}; q_\parallel, q_z) - \sigma^2 G(2,0,2,2\xi_{2s}, 2\eta_{2s}; q_\parallel, q_z)] \\ & - (\lambda_{2s}\delta_{i,2s} + \lambda_{2s}\delta_{j,2s}) P(1+|m_i|+|m_j|, |m_i - m_j|, p_i + p_j, \xi_i + \xi_j, \eta_i + \eta_j; q_\parallel, q_z)|^2, \end{aligned} \tag{15}$$

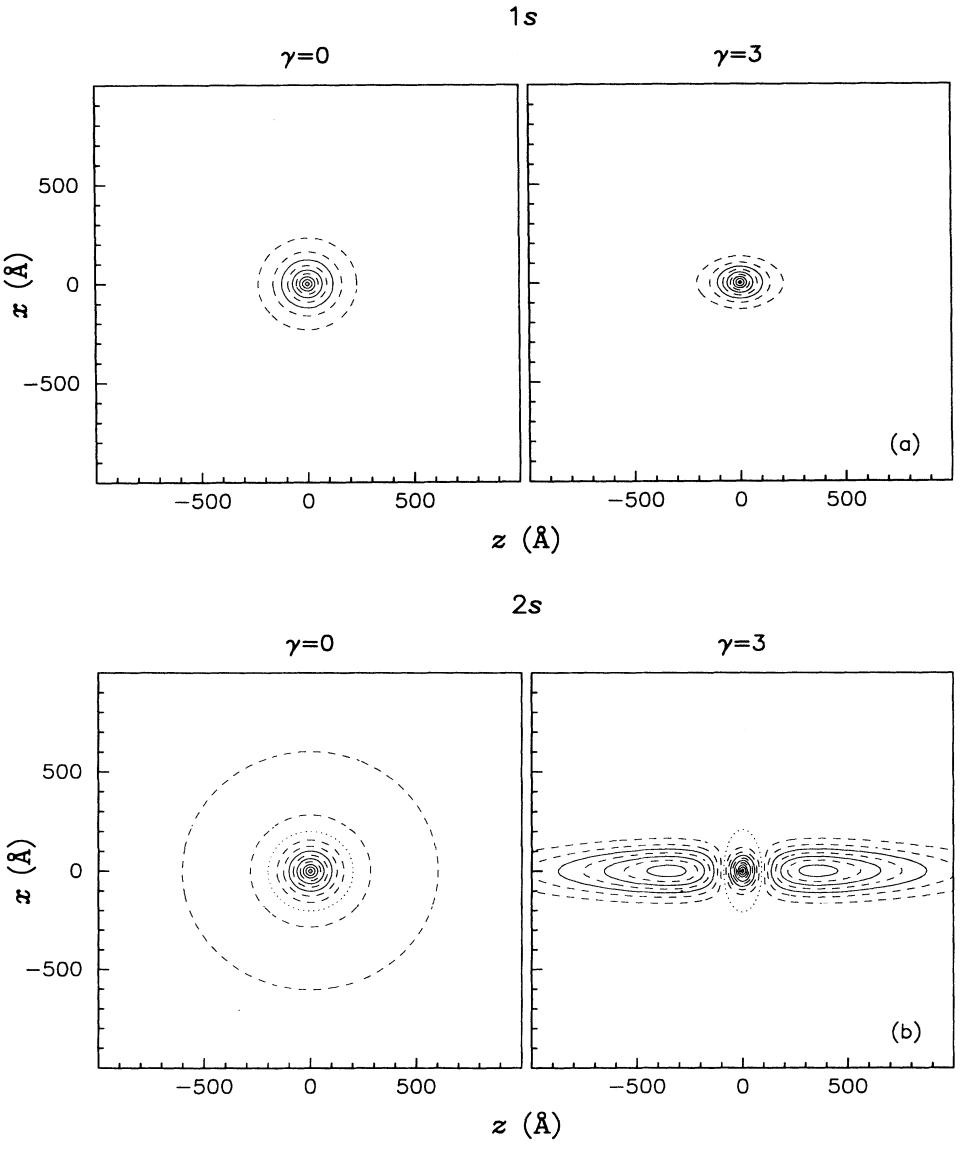

FIG. 2. Electron probability distribution in the x-z plane for magnetic fields $\gamma = 0.0$ (left figures) and 3.0 (right figures) for (a) the $1s$ state, (b) the 2s state, (c) the $2p^{\pm}$ states, (d) the $2p_z$ state, (e) the $3d^{\pm 2}$ states, and (f) the $4f^{\pm 3}$ states.

where we have defined the functions

$$G(\mu,\nu,\lambda,\xi,\eta;q_\parallel,q_z)=\eta\int_0^\infty d\rho\,\rho^\mu J_\nu(q_\parallel\rho)e^{-\xi\rho^2}\frac{\partial^\lambda}{\partial q_z^\lambda}\frac{K_1(\rho\sqrt{q_z^2+\eta^2})}{\sqrt{q_z^2+\eta^2}}, \tag{16}$$

and

$$P(\mu,\nu,\lambda,\xi,\eta;q_\parallel,q_z)=\tfrac{1}{2}\int_0^\infty d\rho\,\rho^\mu J_\nu(q_\parallel\rho)e^{-\xi\rho^2}\int_{-\infty}^\infty dz\,z^\lambda\sqrt{\rho^2+\sigma^2z^2}e^{-iq_zz-\eta\sqrt{\rho^2+z^2}} \tag{17}$$

with ξ_i, η_i, and σ the previously obtained variational parameters, λ_{2s} the orthogonal parameter for the $2s$ state, m_i, p_i the magnetic and z-parity quantum numbers respectively, $J_\nu(z)$ the real and $K_1(z)$ the imaginary argument Bessel functions.

Since $H_I^{i,j}$ represents the transition probability between the $|j;\mathbf{q}\rangle$ and $|i;\mathbf{0}\rangle$ states, the value of it is a measure of how strong the electron-phonon interaction couples these states with each other. In Fig. 5 the numerical results for the 24 matrix elements of $H_I^{i,j}$, which are relevant to the present work, [in units of $(R^*)^2$] are presented as a function of the magnetic field. Notice that (1) most of the values of $H_I^{i,j}$ increase with increasing magnetic field, which can be understood as follows: in-

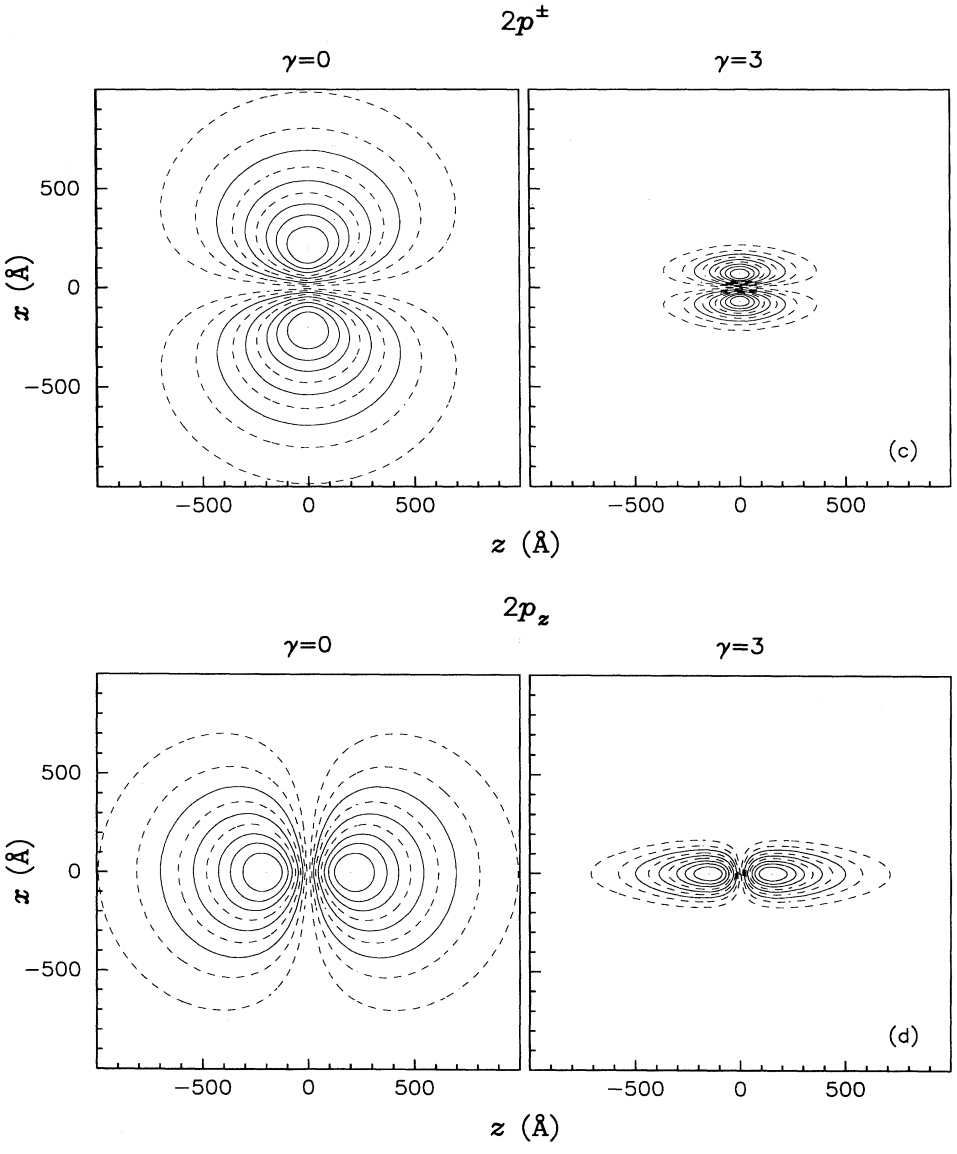

FIG. 2. (*Continued*).

creasing the magnetic field will bind the electron nearer to the donor center and increases the overlap of the wave functions; (2) but the values of $H_I^{2s,j}$ for $j \neq 2s$ and $j \neq 2p_z$ (dotted curves) decrease with increasing magnetic field in the magnetic-field region $0.2 < \gamma < 0.8$ because of the rapid increasing of the $2s$ state width in the z direction; (3) the diagonal $H_I^{i,i}$ matrix elements are larger than the nondiagonal ones, and the less localized states have smaller values; (4) the value of the matrix element $H_I^{i,j}$ is smaller when the ith and jth states have a large difference in magnetic momentum and/or energy; and (5) there are some crossings of curves, which are a consequence of different dependences of the width of the different states on the magnetic field (see Fig. 3).

In order to obtain the polaron correction to the donor energy of the ith state one has to include all donor states in the sum $\sum_j$, which is a formidable task. In Ref. 43 we calculated Eq. (14) for a donor in a $GaAs/Al_xGa_{1-x}As$ superlattice including a finite number of states. Recently, we found that in the small magnetic field region this approach is unsatisfactory and underestimates the polaron correction. Nevertheless, it is possible to evaluate Eq. (14) approximately in such a way that one needs to know only a few relevant states to calculate the polaron shift to the donor energy levels.[52,14] Following the method used in Ref. 52 we iterate the identity

$$\frac{1}{\hbar\omega_{\rm LO} + E_j^0 - E_i^0 - \Delta_i} = \frac{1}{\hbar\omega_{\rm LO} + q^2} - \frac{E_j^0 - E_i^0 - q^2 - \Delta_i}{(\hbar\omega_{\rm LO} + q^2)(\hbar\omega_{\rm LO} + E_j^0 - E_i^0 - \Delta_i)}$$

twice in Eq. (14) and after some analytic calculation we obtain

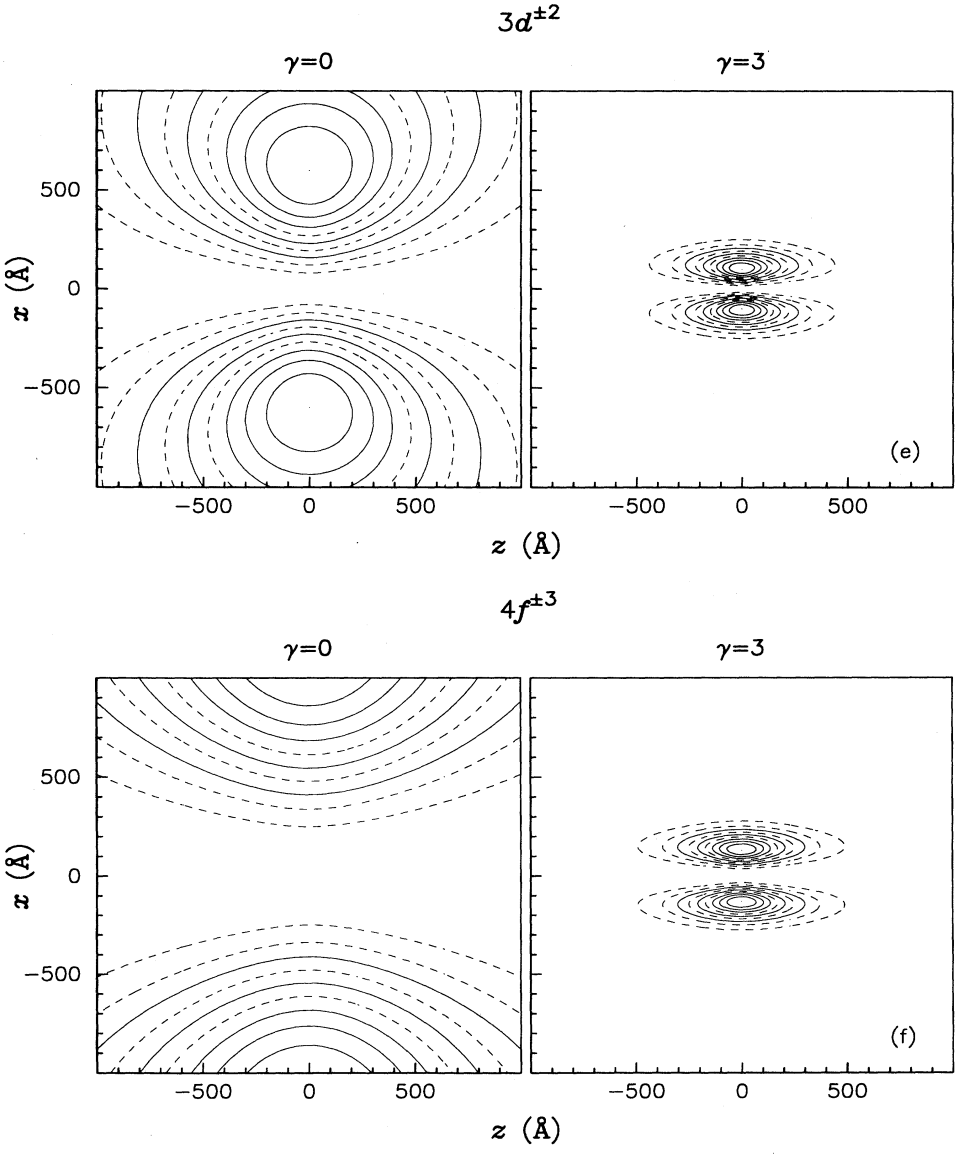

FIG. 2. (*Continued*).

$$\Delta E_i = -\alpha\hbar\omega_{\rm LO} - \sum_j \sum_{\mathbf{q}} \frac{|\langle j;\mathbf{q}|H_I|i;\mathbf{0}\rangle|^2 (E_j^0 - E_i^0 - q^2 - \Delta_i)^2}{(\hbar\omega_{\rm LO} + E_j^0 - E_i^0 - \Delta_i)(\hbar\omega_{\rm LO} + q^2)^2}, \tag{18}$$

which consists of two terms: the first $-\alpha\hbar\omega_{\rm LO}$ is the polaron shift of a free electron in the absence of a magnetic field, and the second contains the correction due to the magnetic field and depends on the specific donor state. The calculation of the polaron correction to the energy of the donor state is reduced to evaluate the second term on the right-hand side of Eq. (18).

A. Nonresonant region

In this region no single term in the sum $\sum_j$ dominates, and consequently a large number of states contribute to the sum $\sum_j$ in Eq. (18). In general, limiting this sum to a finite number will underestimate the polaron correction. For the ground state Platzman[52] found an upper bound to ΔE_{1s} where he was able to formally include all the intermediate states $|j\rangle$ in the calculation. Cohn, Larsen, and Lax[29] have extended this approach to the excited states, but only three lowest states ($1s$, $2p^{\pm}$) were included in the sum $\sum_j$ for the $2p^+$ states. In this paper, we have further extended this method to even higher excited states. Using the three quantum numbers (n,m,p) of the ith state we found

$$\Delta E_{nmp} = -\alpha(\hbar\omega_{\rm LO} + S) \tag{19}$$

with $S = \frac{2}{3}\langle nmp|H_e + \frac{2}{r}|nmp\rangle$ which is found to be equal to

$$S = \frac{2}{3}\left(E^0_{nmp} + \frac{2C_{nmp}}{\langle nmp|nmp\rangle}\right), \tag{20}$$

where E^0_{nmp} is the unpertubed energy of the (n,m,p) state obtained by the variational calculation, and the function C_{nmp} is given by

$$C_{nmp} = Q(|m|,p,-1) \tag{21}$$

for all the considered states with the exception of

$$C_{2s} = 4\pi \int_0^\infty d\rho\, \rho e^{-2\xi\rho^2} \int_0^\infty dz\, e^{-2\eta r}\frac{1}{r} \times \left(1 - \lambda_{2s}\sqrt{\rho^2+\sigma^2 z^2}\right)^2. \tag{22}$$

Equation (19) turns out to be a good approximation to Eq. (18) for all the considered states, with the exception of $2p^+$, and that for arbitrary magnetic fields. Equation (19) is obtained by noticing that for the ith state with the energy E_i^0 below the lowest (i.e., $N=0$) Landau level we have the following: (1) $|E_j^0 - E_i^0| \ll \hbar\omega_{\rm LO}$ in low magnetic fields, and (2) $|E_j^0 - E_i^0| \ll \hbar\omega_{\rm LO}$ or $E_j^0 - E_i^0 > 0$ in high magnetic fields, which implies that $\hbar\omega_{\rm LO} + E_j^0 - E_i^0$ in the numerator of Eq. (18) can be replaced by $\hbar\omega_{\rm LO}$ ($\Delta_i = 0$ for $i \neq 2p^+$). This approximation allows us to perform the sum $\sum_j$ and consequently to formally include all donor states in the calculation. Notice that (1) for $|nmp\rangle = 1s$ Eq. (19) is a rigorous upper bound to the polaron correction of the ground state; (2) this equation is also an accurate approximation to the polaron correction of the excited states, and it is able to give the

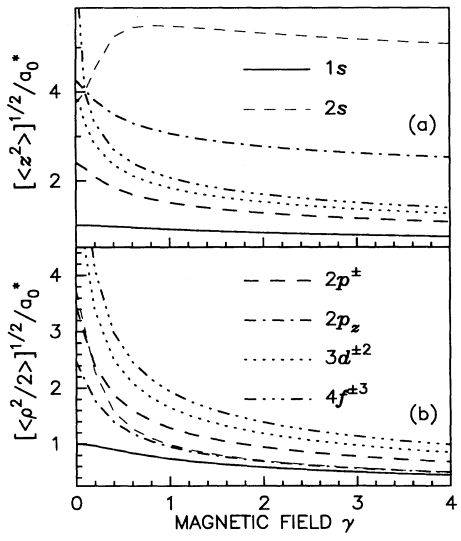

FIG. 3. The widths of the donor wave functions in the z direction (upper figure) and in the x-y plane (lower figure) in units of a_0^* and as a function of the magnetic field for the $1s$ (solid curves), $2s$ (thin-dashed curves), $2p^{\pm}$ (dashed curves), $2p_z$ (dash-dotted curves), $3d^{\pm 2}$ (dotted curves), and $4f^{\pm 3}$ ($-\cdots-$) states.

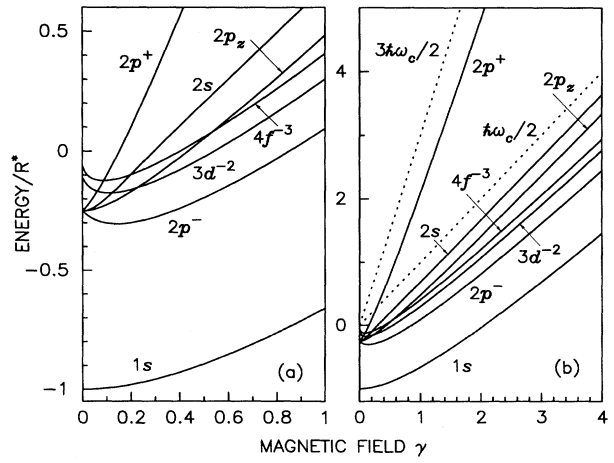

FIG. 4. The energy levels of a donor in GaAs (in units R^*) as a function of the magnetic field (solid curves). In (b) the dotted curves indicate the two lowest Landau levels, and in (a) the small magnetic field region of (b) is enlarged.

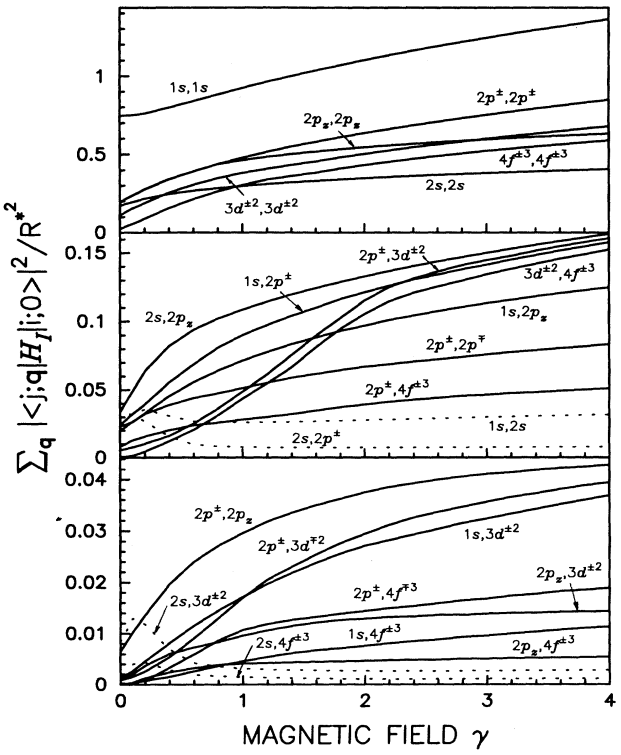

FIG. 5. The values of the electron-phonon transition matrix elements, $H_I^{i,j}$, in units of $(R^*)^2$ are plotted as a function of the magnetic field in GaAs.

maximum polaron correction to the transition energies in the nonresonant region. For example, at $\gamma = 0$ the calculated results for the $1s \rightarrow 2p$ transition energy are 4.200 meV without polaron correction, and 4.389 meV when this correction is included (when we include also band nonparabolicity it will become 4.409 meV) which compares to the experimental result 4.401 meV; and (3) this approach breaks down near the polaron resonant region where the difference between the energies of two donor states is nearly equal to the energy of a LO phonon.

B. Polaron resonant region

When the $1s \rightarrow 2p^+$ transition energy is near the energy of a LO phonon, there may exist a donor state $|j\rangle$ such that

$$\hbar\omega_{\rm LO} + E_j^0 - E_{2p^+}^0 - \Delta_{2p^+} \approx 0,$$

and consequently it will give a dominant contribution to the sum $\sum_j$ of the second term on the right-hand side of Eq. (18). Therefore it will be sufficient to limit the sum $\sum_j$ to these states which are close to resonance. Since the experimental results of Ref. 39 are done in an energy range of the six lowest branches of the $1s \rightarrow 2p^+$ transition it is sufficient to include the $1s$, $2s$, $2p^{\pm}$, $2p_z$, $3d^{-2}$, and $4f^{-3}$ states in our calculation. The matrix elements which we have to calculate are analogous to those in Eq. (15) with the exception that now the integrand has to be multiplied by a factor of $(E_j^0 - E_i^0 - q^2 - \Delta_i)^2/(\hbar\omega_{\rm LO} + q^2)^2$. In the actual calculation Δ_i has been neglected in this factor because it is unimportant. Nevertheless it is included in the numerator of Eq. (18) where it is very important.

However, the above calculation underestimates the polaron correction to the energy of the $2p^+$ state in low magnetic fields, i.e., in the polaron nonresonant region. As a consequence, it leads to a larger $1s \rightarrow 2p^+$ transition energy in the low magnetic field region. A good approximation to the polaron correction Eq. (14) for the $2p^+$ state should have the following properties: (1) at $B = 0$ T the polaron correction should be identical to the one of the $2p^-$ state because in this limit both states are identical; (2) for $B > 0$ T the polaron correction $|\Delta E_{2p^+}|$ should be larger than that to the $2p^-$ state as we infer from the analogy between the $(2p^-, 2p^+)$ states and the free electron $(N = 0, N = 1)$ states; and (3) at resonance, it must give the correct resonant position. At present we are not aware of any simplified expression to Eq. (14) which has these properties. Based on physical intuition we propose the following approximation to Eq. (14) for the polaron correction to the $2p^+$ state:

$$\Delta E_{2p^+} = \Delta E_{2p^-} - \sum_{i=2p^{\pm}} \sum_j \sum_{\mathbf{q}} \frac{m_i |\langle j;\mathbf{q}|H_I|i;\mathbf{0}\rangle|^2 (E_j^0 - E_i^0 - q^2)^2}{(\hbar\omega_{\rm LO} + E_j^0 - E_i^0 - \Delta_i)(\hbar\omega_{\rm LO} + q^2)^2}, \tag{23}$$

which satisfies the above three properties. The second term on the right-hand side of Eq. (23) is zero for $B \rightarrow 0$ and we obtain $\Delta E_{2p^+} = \Delta E_{2p^-}$ as it should be. ΔE_{2p^-} is the nonresonant polaron correction and is given by Eq. (19). For $B \neq 0$ T we include the polaron correction in the form of Eq. (18) as is apparent from the $i = 2p^+$ term in the second term on the right-hand side of Eq. (23), where $m_i = m_{2p^+} = +1$ is the magnetic quantum number of the $2p^+$ state. In doing so we overestimate the polaron correction because this term not only describes the resonant polaron correction but also contains a nonresonant contribution. In order to correct for this we subtract the $2p^-$ polaron correction which is nonresonant in the form of Eq. (18), which is the $i = 2p^-$ term in Eq. (23) with $m_i = m_{2p^-} = -1$. In doing so the constant $-\alpha\hbar\omega_{\rm LO}$ term in Eq. (18) cancels. The sum $\sum_j$ in Eq. (23) can now be limited to the relevant donor states as determined by the energy range of the experiment.

We depict in Fig. 6 the energy levels of the $1s$, $2s$, $2p^{\pm}$, $2p_z$, $3d^{-2}$, and $4f^{-3}$ states together with the same levels

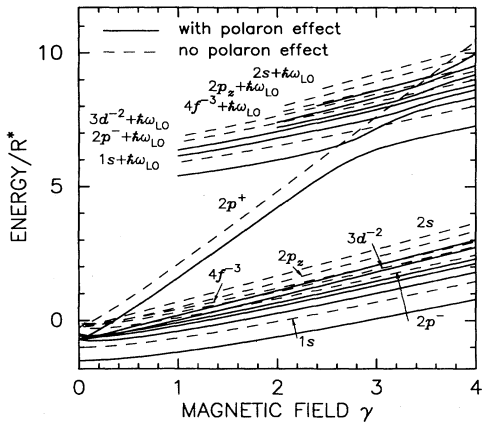

FIG. 6. Energy levels of a donor in GaAs as a function of the magnetic field with (solid curves) and without (dashed curves) the electron-phonon interaction.

shifted over a LO phonon energy (dashed curves) and the levels corrected by the polaron effect (solid curves) versus magnetic field for a donor in GaAs, where the results with polaron correction for the $2p^+$ state are from the method described in Sec. III B and those for the other states are from Sec. III A. Notice that (1) for not too large magnetic fields the polaron correction shifts the energy levels to lower energy, and these shifts increase with increasing magnetic field strength; and (2) at resonance, i.e., $E^0_{2p^+} = E^0_i + \hbar\omega_{\rm LO}$ for $i \neq 2p^+$, there is a crossing of the unperturbed levels. The electron-phonon interaction will lift this degeneracy, and lead to a splitting of these energy levels.

Figure 7 shows the actual polaron shifts $E^0_i - E_i = -\Delta E_i$ of the energy levels of the donor in low magnetic fields (i.e., below the resonant region) where the first term in Eq. (18) ($\alpha\hbar\omega_{\rm LO}$, dotted line) is indicated for reference. $-\alpha\hbar\omega_{\rm LO}$ is the polaron shift of a free electron at $B = 0$ T. From Eq. (18) one can easily prove that $|\Delta E_i| \geq \alpha\hbar\omega_{\rm LO}$ which is clearly satisfied as seen from Fig. 7. The physical reason is that localization of the electron wave function in space increases the polaron correction. The present

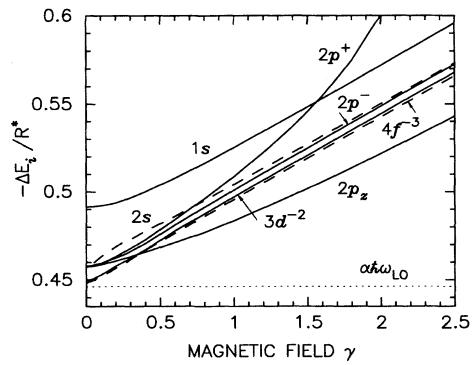

FIG. 7. Shifts of the energy levels due to the electron-LO phonon interaction vs the magnetic field for donors in GaAs.

donor electron is more localized than a free electron and consequently will have a larger polaron binding energy. Increasing the magnetic field decreases the width of the electron wave function (see Figs. 2 and 3) which explains why $|\Delta E_i|$ is an increasing function of γ. Notice that (i) the $1s$ state has the largest polaron correction for $\gamma < 1.5$ because it is the most localized state; (ii) the polaron corrections to the energies of the four states with the principal quantum number $n = 2$ are almost the same at $\gamma = 0$: $\Delta E_{2s} = -0.457\,59R^*$, $\Delta E_{2p^\pm} = -0.457\,57R^*$, and $\Delta E_{2p_z} = -0.457\,36R^*$; (iii) the $2s$ and $2p_z$ states have a weaker dependence on the magnetic field because the width of their wave functions (see Fig. 3) depends less strongly on the magnetic field; (iv) the $2s$ state has a larger polaron correction than the $2p^-$ and $2p_z$ states because most of its probability density is closer to the donor center [see Fig. 2(b)]; and (v) the rapid increase of the polaron correction of the $2p^+$ state for $\gamma > 1.5$ is a result of the fact that this state approaches resonance.

IV. COMPARISON WITH EXPERIMENTS

In this section we compare our theoretical calculation with available experimental results. In the experiment, the sample should be mounted in the Faraday configuration ($\mathbf{E} \perp \mathbf{B}$), i.e., the electric component of the electromagnetic field is perpendicular to the externally applied magnetic field, so that transitions from the ground state to final states with $p = even$ can be observed. For other transitions it should be in the Voigt configuration ($\mathbf{E} \parallel \mathbf{B}$).

First we consider the experimental results in relatively low magnetic fields, where there is no resonant polaron interaction and the electron-phonon interaction only induces a shift of the energy levels of the donor states. In Fig. 8 we show our theoretical results for the transition energies of $1s \rightarrow 2s$, $2p^\pm$, $2p_z$, and $3d^{-2}$ as a function of the magnetic field ($0 \leq \gamma \leq 1$) with (solid

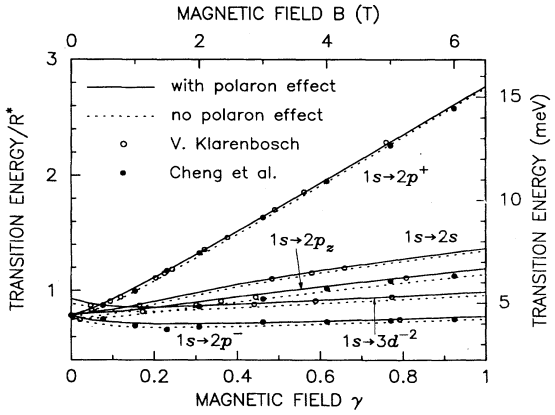

FIG. 8. The $1s \rightarrow 2s$, $2p^\pm$, $2p_z$, and $3d^{-2}$ transition energies with (solid curves) and without (dotted curves) polaron corrections for a donor in GaAs as a function of the magnetic field. The experimental data are from Van Klarenbosch (open circles, Ref. 28) and Cheng *et al.* (solid dots, Ref. 39).

curves) and without (dotted curves) electron-phonon interaction, and compare them with the experimental data of Klarenbosch[28] (open circles) and Cheng *et al.*[39] (solid dots). In the calculation of the polaron correction we have used Eq. (23) for the $2p^+$ state and Eq. (19) for all the other states. It is apparent from this figure that (1) the polaron effect slightly increases the transition energies. This is due to the fact that the polaron correction to the ground state is larger than that to the excited states (see Fig. 7); (2) the polaron corrections to the $1s \rightarrow 2s$, $2p^-$, $3d^{-2}$ transition energies are almost constant with increasing magnetic field, which is due to the fact that the polaron corrections to these states have almost the same dependence on magnetic fields; but the polaron correction to the $1s \rightarrow 2p_z$ transition energy increases with increasing magnetic field because the dependence of the polaron effect of the $2p_z$ state on the magnetic field is weaker than that of the $1s$ state; and (3) two "forbidden" transitions, $1s \rightarrow 2s$ and $1s \rightarrow 3d^{-2}$ were observed in Ref. 28 [$L_i - L_f = \pm 1$ or $L_i = L_f \neq 0$, L_i (L_f) is the angular momentum quantum number of the initial (final) state]. The reason why they could be seen in the experiment was explained in Refs. 53 and 54: noncentrosymmetric electric fields at the neutral donor position, which are due to ionized impurities, cause a mixing of donor states with different magnetic quantum numbers m and z-parity quantum numbers p. This mixing causes these initially forbidden transitions to become weakly possible.

In higher magnetic fields resonant polaron interaction can take place, which changes the energy levels of the donor states appreciably near resonance. We compare in Fig. 9 our theoretical results for the $1s \rightarrow 2p^{\pm}$, $2p_z$ transition energies with the experimental data (solid dots) of Cheng *et al.*[39] In this figure the units $R_0^* = R^*$ and $\gamma_0 = \gamma$ have been used as the free-electron physical parameters at $B = 0$ T. Notice that near resonance six branches of the $1s \rightarrow 2p^+$ transition are observed which are a consequence of the liftings of the $E^0_{2p^+}$ and $E^0_i + \hbar\omega_{\rm LO}$ ($i = 1s$, $2p^-$, $3d^{-2}$, $4f^{-3}$, $2p_z$) degeneracies. The results (dashed curves) without polaron correction cannot explain these higher branches of the $1s \rightarrow 2p^+$ transition. The present calculation (dotted curves) with polaron correction confirms the liftings of these energy-level degeneracies. The agreement between theory and experiment is quite good for the lower transition energies (below 20 meV), but it becomes unsatisfactory for the $1s \rightarrow 2p^+$ transition in high magnetic fields $\gamma > 2$. The reason is that for such large energy differences band nonparabolicity becomes important.

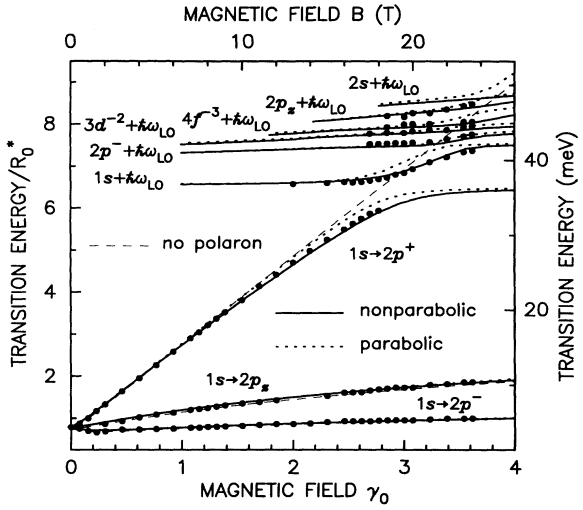

FIG. 9. The $1s \rightarrow 2p^{\pm}, 2p_z$ transition energies as a function of the magnetic field for a donor in GaAs. We compare our theoretical results for the following cases: (a) without the effects of polaron and band nonparabolicity (thin-dashed curves); (b) with polaron correction (dotted curves); (c) including the effects of polaron and band nonparabolicity (solid curves), to the experimental data (solid dots) from Cheng *et al.* (Ref. 39).

We have considered three different expressions for the band nonparabolicity which are available in the literatures.

A. Case 1

We have

$$E_{np} = -\frac{E_g^*}{2} + \left[\left(\frac{E_g^*}{2}\right)^2 + \frac{m_b}{m_e}\left(\frac{m_e}{m_b} - 1 - C^*\right) E_g^* E_p\right]^{1/2} + \frac{m_b}{m_e}(1 + C^*)E_p, \tag{24}$$

where E_{np} and E_p are the donor energies with and without the effect of band nonparabolicity, respectively, $E_g^* = E_g + \Delta_0/3 = 1631$ meV is the spin-orbit-averaged energy gap of GaAs with Δ_0 the spin-orbit splitting energy, and C^* is an adjustable parameter. This expression was obtained by Ruf and Cardona[41] from a simple formula for the bulk Γ_6^c dispersion, and C^* was experimentally determined to be -2.3. If one takes the parameter $C^* = -1$ and neglects the spin-orbit interaction, Eq. (24) will be reduced to

$$E_{np} = \frac{E_g}{2}\left(-1 + \sqrt{1 + \frac{4E_p}{E_g}}\right), \tag{25}$$

which is the well-known Kane's result and has been proven to be a good approximation for the energy of the electron less than 100 meV, which is the region we are interested in. In Ref. 42 this simple expression (25) was

used to successfully describe the band nonparabolicity for free electron cyclotron resonance in GaAs heterostructures.

B. Case 2

We have

$$m^*(E)/m_e = 0.0665 + 0.0436E + 0.236E^2 - 0.147E^3, \tag{26}$$

where $m^*(E)$ is an energy-dependent effective mass of the electron, and E the single electron energy in units of eV. The value of the effective mass at the Γ point is taken to be $m^*(0) = 0.0665m_e$. This expression was obtained by Kolbas,[55] who fitted the following relation, which was first given by Kane[56] using the $\mathbf{k}\cdot\mathbf{p}$ perturbation technique,

$$\frac{1}{m^*(E)} = \frac{1}{m^*(0)} - \frac{5k_BT}{3m^*(0)}\left(\frac{2}{E_g} + \frac{1}{E_g+\Delta_0}\right) \times \left(1 - \frac{m^*(0)}{m_e}\right)^2 \frac{F_{3/2}}{F_{1/2}}$$

to a third-order polynomial in E with k_B Boltzmann's constant, T the absolute temperature, and $F_{1/2}$ and $F_{3/2}$ the standard Fermi intergrals. Although Eq. (26) was deduced at $T = 77$ K, it is generally assumed that this result is also applicable at lower temperatures as the variation of the effective mass with temperature in this range is very small, and furthermore it was claimed that this result is valid in the region $E < 300$ meV.[55,57] This energy-dependent effective mass was discussed in detail in our previous paper[43] for donor energy levels in $GaAs/Al_xGa_{1-x}As$ superlattices.

C. Case 3

We have

$$E_{np} = E_p\left(1 - \delta\frac{E_p}{E_g}\right), \tag{27}$$

where δ is an adjustable parameter. This expression is easily obtained from an expansion of $(1+4E_p/E_g)^{1/2}$ in Equation (25) to second-order in $(4E_p/E_g)$ and then introducing a parameter δ whose value is determined from a comparison with experiment. Equation (27) was used before, e.g., by Singleton *et al.*,[44] who obtained a good fit to their experimental results with $\delta = 1.4$.

The corrections due to the effect of band nonparabolicity should be done on *three* levels: (i) on the unperturbed energies E_i^0 of the donor, (ii) on the effective Rydberg R^* which depends on the effective mass of the electron, and (iii) on the dimensionless unit of the magnetic field γ which decreases with increasing effective mass of the electron. Explicitly this implies that (1) first we defined

$$\frac{1}{m_{np}} = \frac{1}{\hbar^2 k}\frac{dE_{np}(k)}{dk} \tag{28}$$

the dynamical effective mass, where $E_p = \hbar^2k^2/2m_b$ was used in the expressions of E_{np} as an approximation; (2) we took E_i^0, which was obtained from the parabolic band, as E_p into Eqs. (24)–(28) to calculate the energy E_{np} and the effective mass m_{np} of the electron with band nonparabolicity. This method is able to give the transition energies as accurate as those from a self-consistent calculation described in Ref. 43 which is very computer-time-consuming; and (3) we took half of the cyclotron resonant energy of a noninteracting electron to calculate the effect of band nonparabolicity on γ since it is defined as $\gamma = \frac{1}{2}\hbar\omega_c$ in units of R^*.

The numerical results for the $1s \to 2p^{\pm}$, $2p_z$ transition energies corrected by the polaron effect and including the effect of band nonparabolicity are given in Fig. 9 by the solid curves. We used case 1 for the expression of band nonparabolicity because it is the latest experimentally verified expression; case 2 is valid for higher temperature and case 3 is a simplified form of case 1. It is apparent that (1) in very low fields the effect of band nonparabolicity increases slightly the transition energies; for example, at $\gamma = 0$ it (case 1) shifts the $1s \to 2p$ transition energy by 0.02 meV to higher energies which is mainly a consequence of the increase of R^* due to the increase in electron mass; (2) at higher magnetic fields band nonparabolicity decreases the transition energy which is a consequence of the larger energy difference between the initial and final states. Band nonparabolicity diminishes the energies of the higher excited states more than the energy of the ground state; (3) the expression (24) (i.e., case 1) gives the best results, while Eq. (26) (i.e., case 2) underestimates slightly band nonparabolicity, and Eq. (27) (i.e., case 3) significantly overestimates this effect if we use $\delta = 1.4$ as was done in Ref. 44. At $B = 18$ T the theoretical results for the lowest branch of the $1s \to 2p^+$ transition are as follows: 33.03 meV for case 1, 33.94 meV for case 2, and 32.19 meV for case 3, which compares to the experimental result 33.23 meV.[39] We have found that the reduced expression of Eq. (24) used by Wu, Peeters, and Devreese[42] is an excellent approximation in the energy region discussed here, which gives 33.032 meV for the lowest branch of the $1s \to 2p^+$ transition energy at $B = 18$ T, which compares to 33.034 meV for Eq. (24). The value $\delta = 1.4$ in case 3 is clearly too large, which is a consequence of the fact that the polaron effect was not correctly included in Ref. 44 and as a result a larger δ value was needed to explain the experimental data. For completeness we used Eq. (27) and fitted δ to the experimental data of Fig. 9 and found that $\delta = 0.85$ gave reasonable results which is consistent with the conclusion of Ref. 42 where $\delta \approx 0.9$ was found. For the lowest branch of the $1s \to 2p^+$ transition energy we found at $B = 18$ T the following values: 33.92 meV for $\delta = 0.4$, 33.18 meV for $\delta = 0.85$, and 32.19 meV for $\delta = 1.4$.

V. DISCUSSION AND CONCLUSION

We have investigated the transition energies of the $1s \to 2s$, $2p^{\pm}$, $2p_z$, and $3d^{-2}$ states for a shallow donor in GaAs in the presence of a magnetic field. The polaron

TABLE III. Comparison of the $1s \rightarrow 2p$ transition energy (in units of meV) at $\gamma = 0$ for different dielectric constants given in Ref. 1, with $\hbar\omega_{\rm LO} = 36.75$ meV and $m_b/m_e = 0.067$, to the measured value (Expt.) (Ref. 39). E_0 is the result without any correction, E_P includes the polaron effect only, and $E_{\rm PB}$ with polaron and band nonparabolicity corrections.

ϵ_0	R_0^*	$\epsilon_0/\epsilon_\infty$	α	E_0	E_P	$E_{\rm PB}$	Expt.
		1.183	0.071		4.58	4.60	
12.75	5.60	1.166	0.065	4.20	4.20	4.22	
		1.178	0.069		4.45	4.47	
Present		1.174	0.068	4.20	4.39	4.41	4.40
		1.183	0.069		4.17	4.19	
13.18	5.24	1.166	0.063	3.93	3.81	3.83	
		1.178	0.067		4.05	4.07	

correction to these energies is included in our calculation within second-order perturbation theory. We found that (1) the electron-LO phonon interaction always shifts the transition energies to higher values for $1s \rightarrow 2s$, $2p^-$, $2p_z$, and $3d^{-2}$; and (2) it increases the values of the $1s \rightarrow 2p^+$ transition energy in low fields and results in resonant splitting of the energies in high magnetic fields. In order to correctly explain the experimental data, band nonparabolicity has to be included. Our calculation, which *does not contain any fitting parameters*, is in very good agreement with the experimental data given in Refs. 28 and 39.

The experimental measurement for the static dielectric constant of GaAs at low temperature has an uncertainty region,[1] and also for the high frequency dielectric constant, which is determined from the Lyddane-Sachs-Teller relation $\epsilon_0/\epsilon_\infty = (\omega_{\rm LO}/\omega_{\rm TO})^2$ (Ref. 58) with $\omega_{\rm TO}$ the frequency of the transverse-optical phonon. These values will strongly influence the final calculated results because they are able to change appreciably the values of the effective Rydberg $R^* = e^4 m_b/2\hbar^2\epsilon_0^2$ and the coupling constant $\alpha = e^2\sqrt{m_b/2\hbar\omega_{\rm LO}}(1/\epsilon_\infty - 1/\epsilon_0)/\hbar$ of the electron-phonon interaction. In Table III a detailed comparison is presented for the calculated transition energy $1s \rightarrow 2p$ at zero magnetic field for the different dielectric constants given in Table X of Ref. 1 with the experimental result (Expt.) (Ref. 39). $\epsilon_0 = 13.18$ is the value for $T = 300$ K. Notice that (1) our choice of $\epsilon_0 = 12.75$ and $\alpha = 0.068$ in the present work results in an excellent agreement between theory and experiment when polaron effects are included (E_P); (2) if using the value of ϵ_0 at room temperature (i.e., $\epsilon_0 = 13.18$) the calculated results will underestimate the transition energy by about 10% as compared to the experimental results due to the fact that R^* is about 10% less than that at low temperature; (3) because of the uncertainty in the ratio of $\epsilon_0/\epsilon_\infty$ there is an uncertainty in α which ranges from 0.064 to 0.072, which results in a variation of about 10% difference in $E_{\rm PB}$ which includes the polaron and band nonparabolicity corrections (i.e., $E_{\rm PB}$ varies between 4.22 meV and 4.60 meV for $\epsilon_0 = 12.75$, 3.83 meV and 4.19 meV for $\epsilon_0 = 13.18$ respectively); and (4) the effect of band nonparabolicity is not very important due to the small transition energy at $B = 0$ T.

The value of the electron-phonon coupling constant α influences the splitting of the energy levels at resonance, which ($E_{\rm splitting}$) is defined as the difference between the two lowest branches of the $1s \rightarrow 2p^+$ transition energy. In principle the observation of the magnitude of this splitting can be used to determine experimentally the value of α. Therefore in Fig. 10 we show this splitting for $\gamma = 3$ as a function of the electron-phonon coupling constant, where we have fixed m_b, ϵ_0, and $\hbar\omega_{\rm LO}$ in the expression of α. In order to investigate the influence of different approximations we have given the results (1) for a parabolic band (dashed curve), (2) including band nonparabolicity (solid curve; case 1), and (3) using the YKA approximation for a parabolic band (dotted curve). Notice that (i) the splitting, and consequently the effective electron-phonon interaction, increases with increasing value of α as expected; (ii) band nonparabolicity gives a smaller splitting as compared to the parabolic band case; (iii) the splitting when including band nonparabolicity has a stronger dependence on the coupling constant than that for a parabolic band; and (iv) the YKA approximation underestimates the resonant splitting.

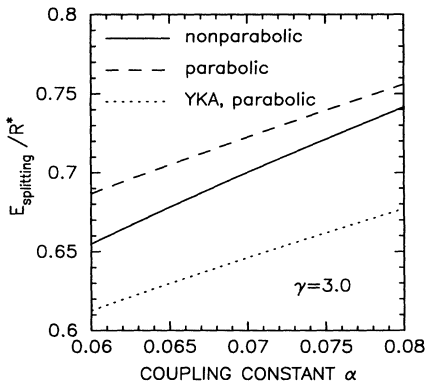

FIG. 10. The splitting of the cyclotron $1s \rightarrow 2p^+$ transition energy at $\gamma = 3$ as function of the electron-phonon coupling constant. We compare the results for (1) parabolic band (dashed curve); (2) including band nonparabolicity (solid curve); and (3) parabolic band within the YKA approximation (dotted curve).

ACKNOWLEDGMENTS

One of us (F.M.P.) is supported by the Belgian National Science Foundation. We are grateful to B.D. McCombe and J.P. Cheng for providing us with the experimental data prior to publication. This work is sponsored by "Diensten voor de Programmatie van het Wetenschapsbeleid" (Belgium) under Contract No. IT/SC/24.

* Also at RUCA, B-2020 Antwerpen, Belgium, and Technical University Eindhoven, The Netherlands.

[1] See, e.g., the review paper by J.S. Blakemore, J. Appl. Phys. **53**, R123 (1982).

[2] W.S. Boyle and R.E. Howard, J. Phys. Chem. Solids **19**, 181 (1961).

[3] H. Hasegawa and R.E. Howard, J. Phys. Chem. Solids **21**, 179 (1961).

[4] F.M. Peeters, J.M. Shi, and J.T. Devreese (unpublished).

[5] R. Cohen, J. Lodenquai, and M. Ruderman, Phys. Rev. Lett. **25**, 467 (1970).

[6] A.J. Rajagopal, C. Chanmugam, R.F. O'Connell, and G.L. Surmelian, Astrophys. J. **177**, 713 (1972).

[7] R.J. Elliott and R. Loudon, J. Phys. Chem. Solids **15**, 196 (1960).

[8] A.G. Zhilich and B.S. Monozon, Fiz. Tverd. Tela (Leningrad) **8**, 3559 (1993) [Sov. Phys. Solid State **8**, 2846 (1966)].

[9] G. Wunner and H. Ruder, Phys. Lett. **A85**, 430 (1981).

[10] H. Ruder, G. Wunner, H. Herold, and M. Reinecke, J. Phys. B **14**, L45 (1981).

[11] V.B. Pavlov-Verevkin and B.I. Zhilinskii, Phys. Lett. **75A**, 279 (1980).

[12] M. Cohen and G. Herman, J. Phys. B **14**, 2761 (1981).

[13] Y. Yafet, R.W. Keyes, and E.N. Adams, J. Phys. Chem. Solids **1**, 137 (1956).

[14] D.M. Larsen, J. Phys. Chem. Solids **29**, 271 (1968).

[15] E.P. Pokatilov and M.M. Rusanov, Fiz. Tverd. Tela (Leningrad) **10**, 3117 (1969) [Sov. Phys. Solid State **10**, 2458 (1969)].

[16] D. Cubib, E. Fabri, and G. Fiori, Nuovo Cimento **10B**, 185 (1972).

[17] H.C. Praddaude, Phys. Rev. A **6**, 1321 (1972).

[18] N. Lee, D.M. Larsen, and B. Lax, J. Phys. Chem. Solids **34**, 1059 (1973).

[19] C. Aldrich and R.L. Greene, Phys. Status Solidi B **F93**, 343 (1979).

[20] D.J. Hylton and A.R.P. Rau, Phys. Rev. A **22**, 321 (1980).

[21] P.C. Makado and N.C. McGill, J. Phys. C **19**, 873 (1986).

[22] D.M. Larsen, Phys. Rev. B **20**, 5217 (1979).

[23] J.M. Chamberlain, P.E. Simmonds, R.A. Stradling, and J.C. Maan, Solid State Commun. **11**, 463 (1972).

[24] E.M. Gershenzon and G.N. Goltsman, Fiz. Tekh. Poluprovodn. **6**, 580 (1972) [Sov. Phys. Semicond. **6**, 509 (1972)].

[25] E.M. Gershenzon, G.N. Goltsman, and A.I. Elmuter, Zh. Eksp. Teor. Fiz. **72**, 1062 (1977) [Sov. Phys. JETP **45**, 555 (1977)].

[26] A.M. Davidson, P. Knowles, P.C. Makado, R.A. Stradling, Z. Wasilewski, and S. Porowski, in *Fundamental Physics of Amorphous Semiconductors,* edited by F. Yonezawa, Springer Series in Solid-State Sciences Vol. 25 (Springer, Berlin, 1981), p. 84.

[27] C.J. Armistead, P.C. Makado, S.P. Najda, and R.A. Stradling, J. Phys. C **19**, 6023 (1986).

[28] A. Van Klarenbosch, Ph.D. thesis, Rijksuniversiteit Leiden, Nederland, 1990.

[29] D.R. Cohn, D.M. Larsen, and B. Lax, Phys. Rev. B **6**, 1367 (1972).

[30] D.M. Larsen, in *Polaron in Ionic Crystals and Semiconductors*, edited by J.T. Devreese (North-Holland, Amsterdam, 1972), p. 237.

[31] G.E. Stillman, D.M. Larsen, C.M. Wolfe, and R.C. Brandt, Solid State Commun. **9**, 2245 (1971).

[32] F.M. Peeters and J.T. Devreese, Phys. Rev. B **31**, 3689 (1985).

[33] P. Pfeffer and W. Zawadzki, Solid State Commun. **57**, 847 (1986).

[34] S.D. Sarma and A. Madhukar, Phys. Rev. B **22**, 2823 (1980).

[35] X.-G. Wu, F.M. Peeters, and J.T. Devreese, Phys. Rev. B **34**, 8800 (1986).

[36] F.M. Peeters, X.-G. Wu, and J.T. Devreese, Solid State Commun. **65**, 1505 (1988).

[37] D.M. Larsen, Phys. Rev. B **30**, 4595 (1984).

[38] M.H. Degani and O. Hipólito, Phys. Rev. B **35**, 7717 (1987).

[39] J.P. Cheng, B. McCombe, J.M. Shi, F.M. Peeters, and J.T. Devreese, Phys. Rev. B (to be published).

[40] G. Ambrazevičius, M. Cardona, and R. Merlin, Phys. Rev. Lett. **59**, 700 (1987).

[41] T. Ruf and M. Cardona, Phys. Rev. B **41**, 10747 (1990).

[42] X.-G. Wu, F.M. Peeters, and J.T. Devreese, Phys. Rev. B **40**, 4090 (1989).

[43] J.M. Shi, F.M. Peeters, G.Q. Hai, and J.T. Devreese, Phys. Rev. B **44**, 5692 (1991).

[44] J. Singleton, R.J. Nicholas, D.C. Rogers, and C.T.B. Foxon, Surf. Sci. **196**, 429 (1988).

[45] W. Chen and T.E. Andersson, Phys. Rev. B **44**, 9068 (1991).

[46] P.V. Allmen, Phys. Rev. B **46**, 15382 (1992).

[47] S. Adachi, J. Appl. Phys. **58**, R1 (1985).

[48] A. Mooradian and G.B. Wright, Solid State Commun. **4**, 431 (1966).

[49] R.F. Wallis and H.J. Bowlden, J. Phys. Chem. Solids **7**, 78 (1958).

[50] M. Shinada, O. Akimoto, H. Hasegawa, and K. Tanaka, J. Phys. Soc. Jpn. **28**, 975 (1970).

[51] G. Lindemann, R. Lassnig, W. Seidenbusch, and E. Gornik, Phys. Rev. B **28**, 4693 (1983).

[52] P.M. Platzman, Phys. Rev. **125**, 1961 (1962).

[53] G.E. Stillman, D.M. Larsen, and G.M. Wolfe, Phys. Rev. Lett. **27**, 989 (1971).

[54] D.M. Larsen, Phys. Rev. B **18**, 535 (1973).

[55] R.M. Kolbas, Ph.D. thesis, University of Illinois at Urbana-Champaign, 1979.

[56] E.O. Kane, J. Phys. Chem. Solids **1**, 249 (1957).

[57] B.A. Vojak, W.D. Laidig, N. Holonyak, Jr., M.D. Comras, J.J. Coleman, and P.D. Dapkus, J. Appl. Phys. **51**, 621 (1981).

[58] R.H. Lyddane, R.G. Sachs, and E. Teller, Phys. Rev. **59**, 673 (1941).